Controlling the profile of high aspect ratio optical gratings in diamond

Ernesto Vargas Catalan[1*], Pontus Forsberg[1], Olivier Absil[2], Mikael Karlsson[1]

[1] Department of Engineering Sciences, Ångström Laboratory, Uppsala University, Box 534, 751 21 Uppsala, Sweden

[2] Département d'Astrophysique, Géophysique et Océanographie, Université de Liège, 17 Allée du Six Août, 4000 Liège, Belgium

[*]ernesto.vargas@angstrom.uu.se

Abstract

Diamond is an excellent material for infrared optics and for applications in harsh environments. Some of those desirable properties, i.e. hardness and chemical inertness, also make it a challenging material to machine and etch. In this study we have tested a wide range of etch parameters in an inductively coupled plasma etcher, in order to produce highly controlled, high aspect ratio gratings in diamond. We discuss the effects of pressure, bias power, and some gas mixture variation (pure oxygen and argon-oxygen) on the etch results and how it impacts the etch mask sputtering and redeposition. We also present a method for applying a fresh aluminum mask, in order to etch even deeper optical gratings. Gratings with aspect ratios as high as 13.5 have been achieved with a 1.42 μm grating period.

Keywords

Grating, reactive ion etching, synthetic diamond, sputtering

1. Introduction

Diamond is a very challenging material to shape, due to its hardness and chemical inertness. Yet diamond has many desirable properties; for optics the broad optical transmission band, high refractive index and high thermal conductivity are of interest. Chemical vapor deposited (CVD) diamond can be used for a wide range of optical applications [1]. Some of these, such as phase masks [2], x-ray sources [3] or diffraction gratings [4], require structures with high aspect ratio and smooth sidewalls. The most successful methods use high density plasmas in inductively coupled plasma reactive ion etching (ICP-RIE) [5]–[7] and Electron-Cyclotron Resonance plasma etching (ECR) [8], [9]. When using highly oxidizing chemistries (O_2 [10], O_2/Ar [9] or Ar/Cl_2 [6]) and high ion energies in these systems it is possible to physically and chemically etch the diamond to some degree. As it is a very slow process, a thick hard mask is required to stand up to the prolonged ion bombardment. When utilizing hard mask for etching, commonly used materials are aluminum (Al) [2], silicon (Si) [5] and SiO_2 [11]. To reach high aspect ratios an iterative process has been developed [12], in which a metal mask is evaporated anew to keep the sidewalls protected and to regenerate the mask.

This study focuses on controlling the angle of the etched sidewall and achieving a steeper wall than in our previous reported work [2]. The goal is to attain higher precision and to have more degrees of freedom when producing micro-optical components. In a deep grating, such as a half wave plate grating [13], good control of the angle becomes every bit as important as the width of the wall. A perfectly vertical sidewall has not been achieved, and is unlikely when the etching is highly dependent on the kinetic energy of impinging ions. Redeposited mask material also has an effect on the sidewall angles in gratings. In order to control this redeposition we previously showed the importance of using a thick mask with vertical edges [2]. Here we develop this masking technique further, as well as vary the pressure, substrate bias power and gas mixture during diamond etching. We also introduce a way of applying fresh mask material to an already etched grating using sputtering and a short etch step, in order to reach even greater etch depths. Our method here is similar to a previously reported one using evaporation at an oblique angle to re-mask a grating [12], but is better suited for curved gratings. In section 2, we will describe the masking process and etching, including all variations of etch parameters, followed by the etch results and discussion in section 3.

2. Experiment

Several preparation steps are needed before the actual diamond etching can occur. Most of these are not the focus for the study, but must still be described, as they are critical parts for the process. We begin with acquiring CVD diamond substrates, which undergo a cleaning process. The diamonds are then ready to be covered in metal layers, through deposition, which will later function as hard masks during the etching. The lithography steps are a bit different from the conventional standard and will thus be explained in full detail in section 2.4. For our pattern transfer process we require a soft stamp, which is copied from a predefined resist pattern made by electron beam (e-beam) lithography, and then simply put on the resist-covered diamonds and left in alcohol vapor. The etching is then carried out in steps to transfer the pattern to the thicker Al layer and then the diamond etching can begin. After etching, the substrates are cracked and mounted in a scanning electron microscope (SEM) for characterization.

2.1 Substrates and pre-cleaning

Polycrystalline CVD diamond substrates of optical quality (Element Six Ltd. and Diamond Materials GmbH) were used in these experiments. The circular substrates were 10 mm in diameter and 300 µm in thickness. In order to evaluate more etch recipes on the same substrate, these were broken in two or four before being used. The substrates were washed in acetone, iso-propanol and water, then cleaned in hot piranha solution (H_2SO_4:H_2O_2) and hydrofluoric/nitric acid (HF:HNO_3). After rinsing in water and iso-propanol, the substrates were blown dry with nitrogen.

2.2 Metal deposition

Masking layers were deposited by magnetron sputtering (Von Ardenne CS 730S). Three layers were deposited in sequence; a thick Al layer, a Si layer and a thin Al layer. The thick Al layer was sputtered at a power of 1000 W for 265 s and the thin one for 30 s. The Si layer was sputtered at a power of 500 W for 375 s. The resulting mask stack had a 1 µm thick Al layer at the bottom, 450 nm of Si in the middle and 100 nm of Al on top. The samples were exposed to air between the depositions of the layers. In this way a thin native oxide is formed in between the mask layers.

2.3 Stamp fabrication

In previously documented experiment [2] a grating pattern, annular with grooves, was used to demonstrate high-aspect ratio structures in diamond. It also showed good reproducibility. In this study the same pattern will be used to determine if higher and lower sidewall angles of the grating structures can be accomplished. The original pattern (also called “master”) is a circular grating with a period of 1.42 µm and a line width of 700 nm. It was written by electron beam (e-beam) lithography in 500 nm thick ZEP resist (Zeon Chemicals) on a 2″ Si wafer. This master pattern was replicated by casting in polydimethylsiloxane (PDMS, Wacker Elastosil RT601). The base and the curing agent were mixed in a 10:1 ratio and a small amount was poured onto the patterned wafer. The wafer was carefully leveled in a laminar flow cabinet (LAF-bench) and left for 20 min, allowing the silicone to spread into a thin layer and for air bubbles to escape. Remaining air bubbles at the surface were removed by gently blowing compressed air over the surface. The wafer was then placed in an oven at 75°C for 25 min to cure the PDMS. Finally, the PDMS stamp was peeled off from the wafer. The process does not damage the master wafer and can be repeated many times. All stamps used here were cast on the same master.

2.4 Solvent-assisted microcontact molding (SAMIM)

In order to transfer the pattern to the diamond substrates a method called solvent assisted microcontact molding (SAMIM) was used. Our method is based on that reported in [14], but differs in that we used a vapor phase solvent and a thin PDMS stamp. S1813 photoresist (Shipley) was mixed with AZ EBR 70/30 solvent (MicroChemicals) in a 1:2 volume ratio and spin coated on top of the sputtered diamond substrate at 6000 rpm for 30 s. After baking on a hot plate at 115° C for 60 s, the resulting resist layer was 200 nm thick. The PDMS stamp was cut to a size somewhat larger than the diamond substrate and placed on top of the resist film. Ethanol (97%) was poured into a large petri dish until it just covered the bottom of the dish. The diamond substrate, with

the PDMS stamp on top, was placed in a smaller petri dish. The smaller dish was then placed open in the larger one, and the lid was put on the larger dish. This left the substrate in ethanol vapor, but without direct contact with the liquid ethanol. PDMS is permeable to ethanol, so ethanol vapor could diffuse through the stamp to reach the thin photoresist film, which is ethanol soluble. As the resist softens it fills the pattern due to capillary forces. After about 30 minutes the PDMS pattern was completely filled. This could be observed as a distinct lowering of the intensity of the diffraction colors from the grating. The PDMS/diamond stack was then removed from the ethanol vapor and the remaining ethanol was baked out by heating it to 60° C for 10 minutes on a hot plate. The PDMS stamp was then gently removed from the diamond substrate leaving a perfect replica of the grating pattern in the resist (see Figure 1).

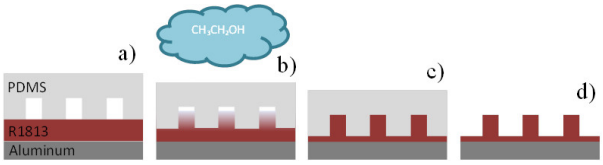

Figure 1: Description of the SAMIM process: a) stamp positioned on resist, b) ethanol vapor dissolves the resist, c) ethanol evaporated during soft bake, d) resist hard baked

The PDMS stamp can be reused, but to avoid contamination a new one was used for each sample in this study. Finally the diamond substrate was hard baked on a hot plate at 115°C for 5 minutes; the patterned resist layer was then 350 nm thick and the residual resist layer at the bottom of the grating pattern only a few nanometers thick. It should be noted that when using SAMIM, as in other micro/nanoimprint methods, it is important to match the fill factor of the micro/nano pattern with the thickness of the spin coated resist. A too thin film will not have enough resist to completely fill the pattern and a too thick one will leave a thick residual polymer layer at the bottom of the pattern. A high residual thickness is unwanted since this will degrade the fidelity of the pattern when it is etched into the underlying substrate.

2.5 ICP etching

An inductively coupled plasma (ICP) etching system (PlasmaTherm SLR) was used for etching all the masking layers as well as the diamond substrate. The system has two etching chambers, one for metal etching, using chlorine chemistry, and the other for Si and diamond etching. Because the etcher was built for wafer scale substrates, the diamond substrate was glued on a 4" Si wafer using Crystalbond 509 (at 90°C on a hot plate) prior to etching. The three masking layers were etched one by one. The thin structured resist layer was used as a mask to etch the pattern into the top Al layer using Cl_2/BCl_3 plasma at a low bias power. The Si layer was then etched using SF_6/C_4F_8/Ar plasma. Here the Al layer was acting as the etch mask. The etch process produces vertical Si sidewalls and it has very little effect on the Al mask, thus over etching was not a problem. Si served as mask for etching the thick Al layer, using two plasma processes that were cycled. In the first step Al was etched in a Cl_2/BCl_3 plasma with strong bias power and in the second step an O_2 plasma with weak bias power oxidized the Al. By cycling these, an Al mask with somewhat rough, but almost vertical sidewalls could be achieved. The etch parameters used for etching the masking layers can be found in
. Before the diamond etch step, the line width was measured by SEM, this to confirm that each test sample had a line width of 700±20 nm.

Table 1: Etch recipes for the masking layers

Recipe	Gas [sccm]	RF power (ICP) [W]	RF power (bias) [W]	Pressure [mTorr]	Time [s]	Note
Thin Al	15 Cl_2, 50 BCl_3	600	30	6	60	Over-etched for 25 s.
Si	10 SF_6, 20 C_4F_8, 70 Ar	825	50	10	210	Does not affect Al-mask
Thick Al	15 Cl_2, 50 BCl_3/ 50 O_2, 20 Ar	600/400	90/10	6/10	6 Cycles + 20 s Al etch step	Cycled (25 s/7 s), purge between steps

The diamond substrates were etched with either Ar/O_2 or pure O_2 plasmas with three different settings for bias and at three different process pressures. The ICP power was kept at 850 W and the wafer cooling was left unchanged. The various diamond etch recipes are described in Table 2.

Table 2: Parameters for diamond etching

Recipe	Gas [sccm]	RF power (bias) [W]	Pressure [mTorr]
ArO_2-22005	40 O_2, 20 Ar	220	5
ArO_2-32005	40 O_2, 20 Ar	320	5
O_2-22005	40 O_2	220	5
O_2-32005	40 O_2	320	5
O_2-42005	40 O_2	420	5
O_2-22010	40 O_2	220	10
O_2-32010	40 O_2	320	10
O_2-22015	40 O_2	220	15

The recipe denoted ArO_2-22005 is the one used in our previous study [2]. The etch process was divided into two steps, one etch step and one cooling step to avoid overheating. The diamond etching step lasted for ten minutes and was followed by a seven and a half minute cooling step (i.e. plasma turned off). This procedure was cycled until the required etch time was reached, usually after four etching cycles. In the case of the highest bias power (420 W), etching was stopped after three cycles to avoid etching through the etch mask. To study the evolution of the etched diamond profile and redeposited aluminum oxide [2] over time, three samples were etched for 10, 20 and 40 minutes, respectively, using the O_2-22005 recipe.

We also carried out an experiment to determine how deep we could etch the grating. This was done by using recipe O_2-32005 or O_2-42005 repeated times, with a depositing step of fresh Al layer on the etched grating in between. A similar method as described in [12] was used. In short, these authors used thermal evaporation of Chromium (Cr) at an oblique angle (from two opposite directions) to re-mask an already etched grating, resulting in the top of the grating to be covered with Cr while the Cr did not reach the bottom of the grating (due to shadowing effects). The diamond etching could then be continued to reach a much deeper grating. In our experiment we instead used sputter deposition of Al to produce a new mask layer (same process as used for the original Al etch mask). Since the shadow effects using sputtering are not as strong as when using evaporation, a thin Al layer will reach the bottom of the grating. Therefore we had to add an additional Al etch step to open up the Al mask in the trenches.

Firstly a diamond grating was fabricated using O_2-32005 for 25 minutes, yielding a depth of 4.4 μm; the etch masking layers and the redeposited aluminum oxide (from the diamond etching process) were completely removed with H_2SO_4:H_2O_2 and HF:HNO_3. A fresh layer of Al was then deposited, using sputtering for 115 s, which gives a 450 nm thick Al layer on a flat surface. As mentioned above, the Al thickness at the bottom of the narrow diamond trench is much lower than on the top of the grating due to shadowing effects. The Al was therefore etched for a very short time (20 s), using the same etch recipe as for the thin Al mask layer (see
). In this way we tried to completely remove the thin Al layer at the bottom of the trenches while the thicker Al film at the top of the grating still covered the diamond surface. The diamond etching was then continued with O_2-32005 in steps of 6 minutes and 15 seconds for 2 cycles. The Al layer was then stripped again and the "re-masking" step was repeated for a total of 8 iterations resulting in a total etch time of 75 minutes. A second test was also performed, using diamond recipe O_2-42005. Due to a faster mask etch rate, a shorter cycling step was chosen (5 minutes). As in the first test, the grating was etched to a depth of 4.4 μm (25 minutes) before the re-masking step. Ten iterations were then used for the re-masking, resulting in a total etch time of 75 minutes.

2.7 Characterization

All samples were measured by imaging the cross section of the etched diamond grating in a SEM (Zeiss, MERLIN). The diamond substrates were cracked perpendicular to the lines in the grating pattern, so that it was easy to measure the width at the top and at the bottom of the diamond walls as well as the depth of the grating. With these values the sidewall angle of the grating structure could be calculated. None of the samples were cleaned prior to SEM imaging, this since we wanted to evaluate the location of redeposited mask material as well

as the shape of the remaining Al mask. Each cross section was imaged two times; one showing four grating periods and the other one – to acquire an overview of the profile and the other showing one grating period so that the redeposition of aluminum oxide could be compared between different etch recipes.

3. Results and discussion

3.1 Profiles of the etched gratings

All etch recipes yielded diamond structures with flat tops and nearly vertical sidewalls, see for measured parameters and Figure 3 for actual etch results. The angle of the etched diamond sidewalls varies between 2.1° to 4.2°, see Table **3**. All fabricated diamond gratings had a line width in the range of 680 to 720 nm and the diamond etching was performed sample by sample.

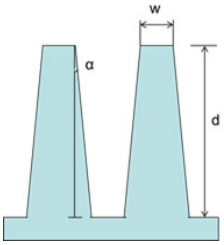

Figure 2: Schematic of an etched diamond grating, illustrating the angle (α), width at the top (w) and depth (d).

Figure 3 shows the cross sections of the fabricated diamond gratings, using the different etch recipes, and Table 3 summarizes the depth of the grating (d), the sidewall angle (α) and line width at the top of the grating (w) as defined in Figure 2.Higher pressure also results in a "double tip" halfway through the etching; it starts to appear at 10 mTorr (Figure 3 f) and is even more prominent at 15 mTorr (Figure 3 h); lower pressures on the other hand yields steeper sidewalls. For both plasma chemistries the etch rate and the etch depth increases as the substrate bias power is raised. Using both high bias power and low pressure resulted in having the redeposited aluminum oxide reach deeper in the trenches. For all etched samples it would still be possible to etch the gratings deeper since neither do the etched sidewalls intersect in a V-shape, nor is the redeposition grown enough to bridge the gap between the gratings. Lowering the pressure and raising the bias even more (not possible using our etch system) might give the possibility to obtain almost vertical walls, thanks to the increase in ion bombardment of the surface during the diamond etching. Lower pressure also gives steeper sidewalls and thinner redeposition layer on the sidewalls; as less collisions occur between incoming ions and sputtered atoms (from the Al layer) compared to having more collisions and therefore forcing the sputtered material downwards.

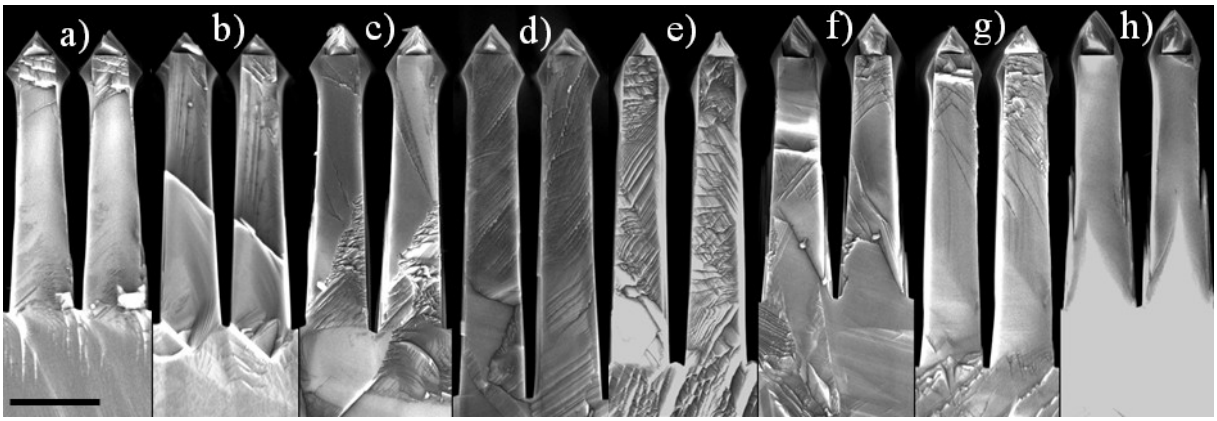

Figure 3: SEM micrographs of the etched diamond gratings cross section using the eight different recipes, a) ArO_2-22005, b) ArO_2-32005, c) O_2-22005, d) O_2-32005, e) O_2-42005, f) O_2-22010, g) O_2-32010 and h) O_2-22015. The scale bar is 2 µm wide. Note that e) has only been etched for 30 min. Compared to the all the others that were etched for full four cycles (40 min).

Table 3: Etch results for the recipes described in Table 2

Etch parameters	top [nm]	bottom [nm]	depth [nm]	angle [degrees]	etch rate [nm/min]
ArO_2-22005	701±9	1272±18	4865±39	3.36±0.10	122
ArO_2-32005	705±17	1244±27	5438±21	2.84±0.17	136
O_2-22005	708±9	1250±36	5059±42	3.06±0.20	126
O_2-32005	703±35	1222±54	6010±108	2.48±0.13	150
O_2-42005[1]	689±17	1119±30	5888±76	2.09±0.14	196
O_2-22010	705±11	1279±35	4481±41	3.66±0.26	112
O_2-32010	713±13	1279±26	6171±70	2.63±0.12	154
O_2-22015	685±5	1334±28	4460±50	4.16±0.21	111

[1] Note that recipe O_2-42005 only was etched for 30 minutes

In Figure 4 we have collected all the values from Table 3 and compared them so that the diagram shows the angle and etch rate dependency for substrate bias power and chamber pressure. The diagram demonstrates that it is possible to control the angle and the final etch depth by adjusting the bias or the pressure.

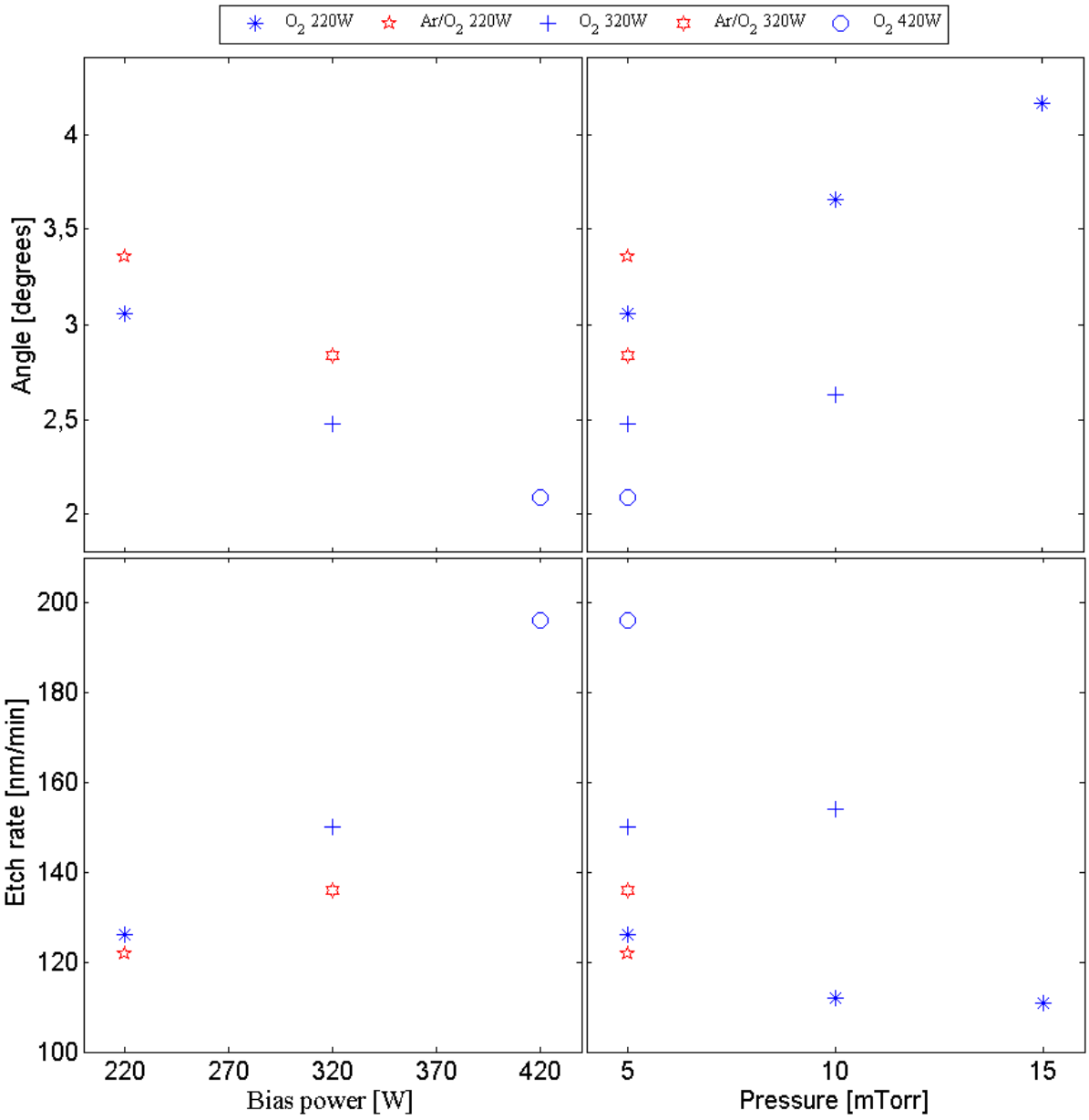

Figure 4 : Diagrams demonstrating trends by grouping all the O_2 and the Ar/O_2 recipes together.

3.2 Redeposition

When etching deep micro/nano-structures in diamond a thick etch mask is needed to ensure that the top of the diamond grating is protected during the whole etching. During the last 15 years, our group has demonstrated a wide variety of diamond micro-optical structures using plasma etching [15], [16] and we have found that using Al as etch mask is generally a good choice. This is mainly due to the relatively high etch selectivity between diamond and Al (50:1) and to the fact that that Al is a well-known etch mask material (easy to process). But since diamond etching in general is a physically dominated etch process (high substrate bias, low pressure), the Al mask tended to be sputtered away, in particular along edges of the mask, and get redeposited on the opposite side of the groove.

A simple two dimensional model was programmed in MATLAB in order to better understand what gives rise to the observed geometries. The model is based on a 2D matrix with non-zero elements representing solid material. In each time step, the top non-zero element in each column may be sputtered, with a probability that depends on the value of the element and the local angle of the surface, as calculated from the surrounding columns. The probability distribution is of a form consistent with sputtering experiments [17]. If the element is sputtered, that

element is set to zero for future time steps. A sputter direction is chosen at random, the distribution again dependent on the surface angle and consistent with experimental results [18]. If a non-zero element is found along a vector in this direction, the element before it is set as a redeposited element. A redeposited element will have a lower probability of being sputtered than the original. This because of our own observation that the redeposited material, presumably oxidized to some degree, is more resistant to sputtering than the original Al mask. Since we did not have data on Al sputtering with O_2, the parameters of the yield and direction distributions were guessed at. We based these guesses on sputtering data of metals with inert ions and our own observations that sputtering increases dramatically at the edge of the mask and the redeposited material appears well focused on the opposite side of the groove.

With this rather naïve and low-resolution model we already get results that are remarkably similar to what we see experimentally (Figure 5). Varying the relative sputter yields of original and redeposited material or the angle dependence in the sputter yield changes the details of the achieved geometry, such as the angle of the mask and the thickness of the redeposition, but it remains qualitatively similar within a wide range in these parameters.

We thus conclude that the triangular cross section of the mask after etching as well as the shape and positioning of the redeposited oxide can be explained simply by the angle dependent sputter yield of the Al mask and the lower sputter yield of the deposited aluminum oxide compared with Al. In these simulations we also see that the redeposition of sputtered mask material plays an important role in reducing the etch rate of the mask.

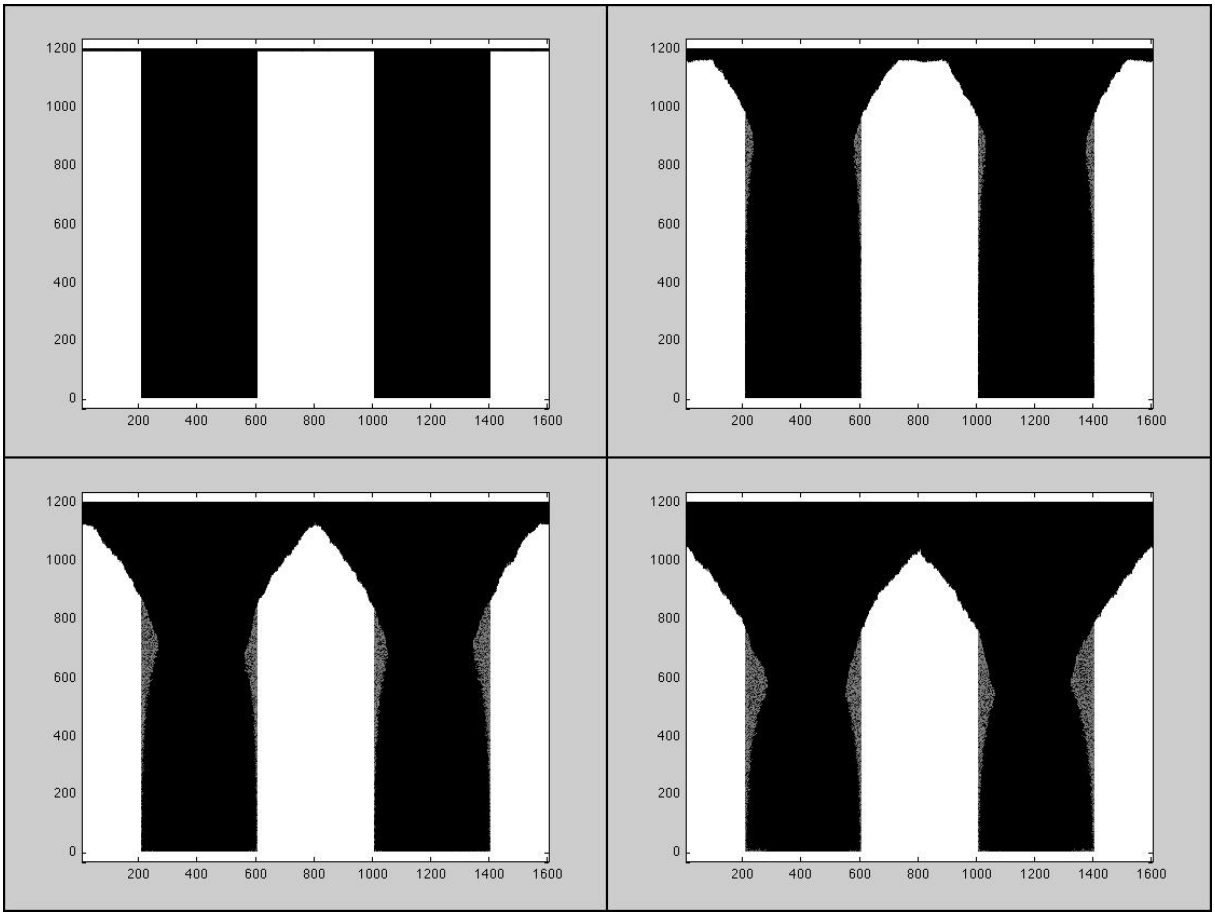

Figure 5: Progression of the simulated mask sputtering. White is initial material, black is vacuum and grey is redeposited material.

Figure 6 shows SEM pictures of the top of the fabricated diamond gratings, where the redeposition can be distinguished from the diamond structure and the remaining Al mask. The effect of this redeposited material is sometimes beneficial and sometimes detrimental to the fabrication of optical structures in diamond. As the oxide not only covers the sidewalls of the etched diamond but also covers the top of the diamond structures, it protects

this area from further etching (which would completely destroy the grating otherwise). But if the redeposition is too strong (thick), it might also prevent the reactive ions from reaching down into the trenches (i.e. the etching stops). From Figure 6 one can infer several characteristics of the various recipes, such as: the redeposition is stronger in the recipes with Ar, and higher process pressure seems to leave the redeposited aluminum oxide closer to the top of the grating. The recipes using pure O_2 has thinner layers of redeposited material covering the sides. Another difference is that the recipes using a high bias leaves the deposited material further down the trench while higher pressure produces more material higher up. Using a high bias and a low pressure (Figure 6 e), we achieve the thinnest redeposition layer, but it is also the one where the aluminum oxide almost covers the entire sidewall (almost down to the bottom of the grating). This recipe is the best candidate (among the evaluated recipes) to obtain the deepest trench. With an even thicker Al mask than the one used in this study, it would be possible to reach a depth of around 8 µm, giving us an aspect ratio of 1:11.

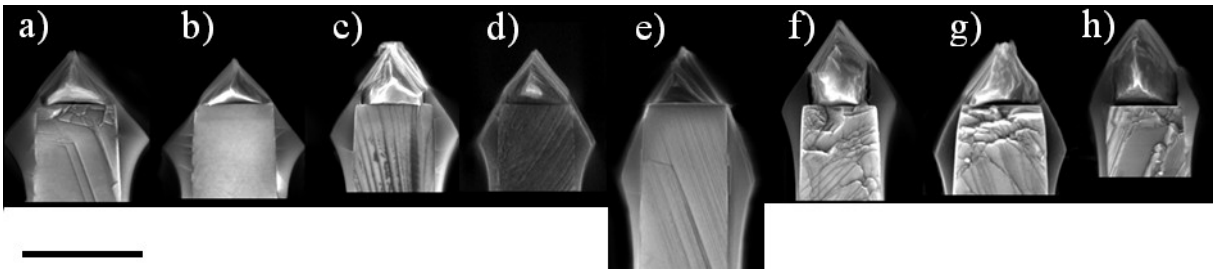

Figure 6: SEM micrographs of the tops of the eight etched diamond gratings, showing the redeposition of aluminum oxide, a) ArO_2-22005, b) ArO_2-32005, c) O_2-22005, d) O_2-32005, e) O_2-42005, f) O_2-22010, g) O_2-32010 and h) O_2-22015. The scale bar is 1 µm wide.

3.3 Etching as a function of time

To be able to see how the Al mask and the diamond grating evolve during the diamond etching, three samples were etched for 10, 20 and 40 minutes respectively (see Figure 7). The different cross sections show that the Al mask profile changes over time. After 10 minutes of etching, the thick Al layer has started to deform, but no sputtered material is yet seen. After 20 minutes, the mask layer has changed profile and is now more triangular, the sides are also covered with aluminum oxide, which is decreasing the gap between the grating sidewalls. The depth is now almost twice as large and the bottom is flatter. After 40 minutes, the sputtered Al layer has redeposited further down and started to close the gap. The depth is now almost a three times deeper than after 10 minutes, which means that the etch rate decreases as the size of the opening shrinks.

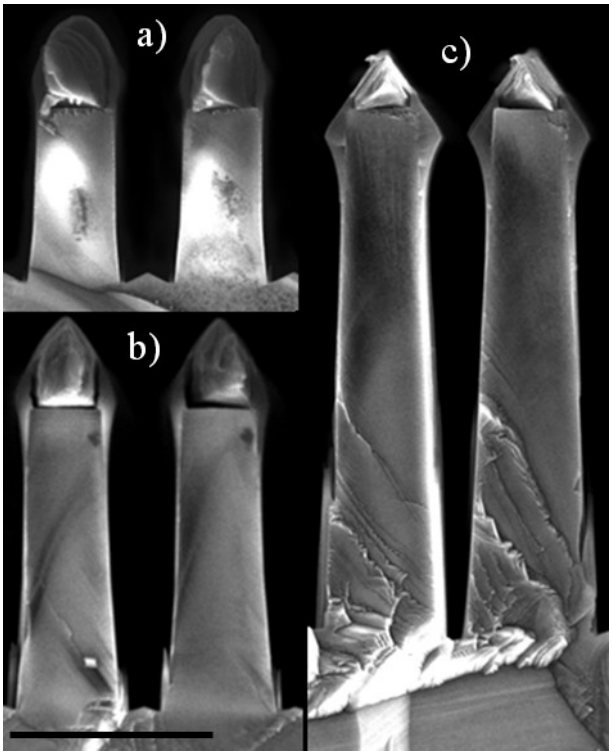

Figure 7: SEM picture showing the cross section of diamond grating etched with O2-22005 for an etch time of a) 10, b) 20 and c) 40 minutes. The scale bar is 1 µm wide.

3.4 Increasing the etch depth by periodically renewing the Al mask

Sputtering Al on an already etched diamond grating resulted in an Al film that was thicker at the top (about 500 nm) than at the bottom (about 20 nm) due to shadowing effects. Along the sidewalls, the Al film was quite thick at the top but thinning quickly with depth. After a short Al etch (20 s) using the same recipe as for the thin Al etch, the bottom of the trenches was clear of Al, while there was still a significant Al layer on top of the grating (see Figure 8 a).

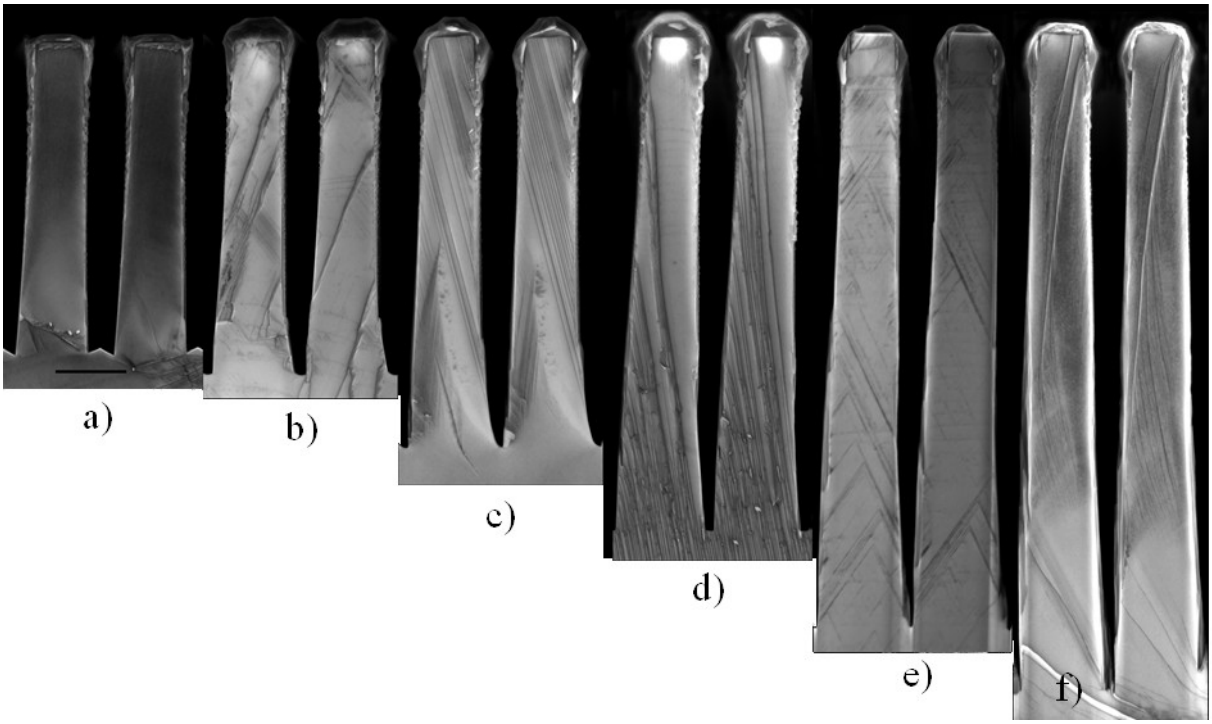

Figure 8: a) Pre-etched diamond grating with a depth of 4.4 µm, b) first iteration 5.19 µm, c) second iteration 5.86 µm, d) fourth iteration 7.27 µm, e) eighth iteration 8.66 µm and f) tenth iteration 9.55 µm. The scale bar is 1 µm wide.

The first etch step was stopped after 6 minutes 25 seconds. The sample was then cracked to determine the diamond etch rate and to see if the deposited Al layer was thick enough to protect the flat top, which was the case. The diamond grating was subsequently etched again, cracked and analyzed by SEM (Figure 8 b). The grating depth had now increased to 5.19 µm, still showing a nice grating profile. Therefore a series of three new Al deposition/Al etching/diamond etching steps was performed, as illustrated in Figure 8. Since the sidewall angle decreases, an even deeper trench (depth 9.5 µm, angle 1.75° and aspect ratio 12.9) than originally expected can be reached. This method was also evaluated using O_2-42005, yielding a final etch depth of 10.0 µm, an angle of 1.55°, and an aspect ratio of 13.5. The only difference is that the diamond etch steps were divided into 5 minutes (or multiples of it) due to the more aggressive etch process with respect to the Al mask. Figure 9 shows SEM images of the etched gratings, while Table 4 lists all the experiments carried out and their results.

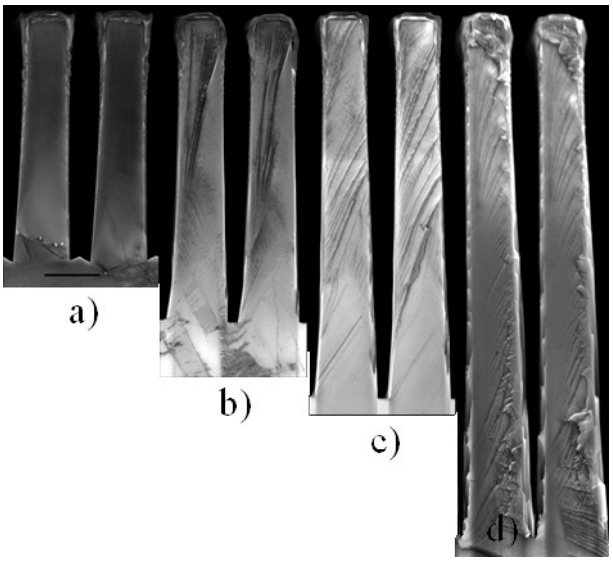

Figure 9: a) Pre-etched diamond grating with a depth of 4.4 µm, b) second iteration with 5.85 µm depth, c) fourth iteration with 7.37 µm depth and d) tenth iteration with 9.99 µm depth. The scale bar is 1 µm wide.

By plotting the etch rate versus the aspect ratio of the etched grating (see Figure 10), it is shown that reaching aspect ratios greater than 14 is a challenge (with a line width of 700 nm and period of 1.42 µm) because the etch rate, at this point, starts to dramatically decrease. The etch rate slows down dramatically as the profile approaches a "V"-shape, in this case around 10 µm in depth (assuming a sidewall angle of 1.55°). One important feature emerges when comparing the redeposited aluminum oxide profile in Figure 7 with Figure 8 or Figure 9, in the original process; the Al mask layer is redeposited on the neighboring grating and grows over time. With the removal and renewal of the Al mask, the Al mask profile is almost kept the same during etching and the gap between the gratings does not shrink. Also for both recipes used in this study the sidewall angle increase in the beginning of the etching but as the etching proceed the angle starts to decrease, see Table 4. This is credited to the fact that after each renewal of the Al mask, the gap between the gratings is almost restored to its original geometry allowing the incoming ions to etch the previously aluminum oxide protected sidewall.

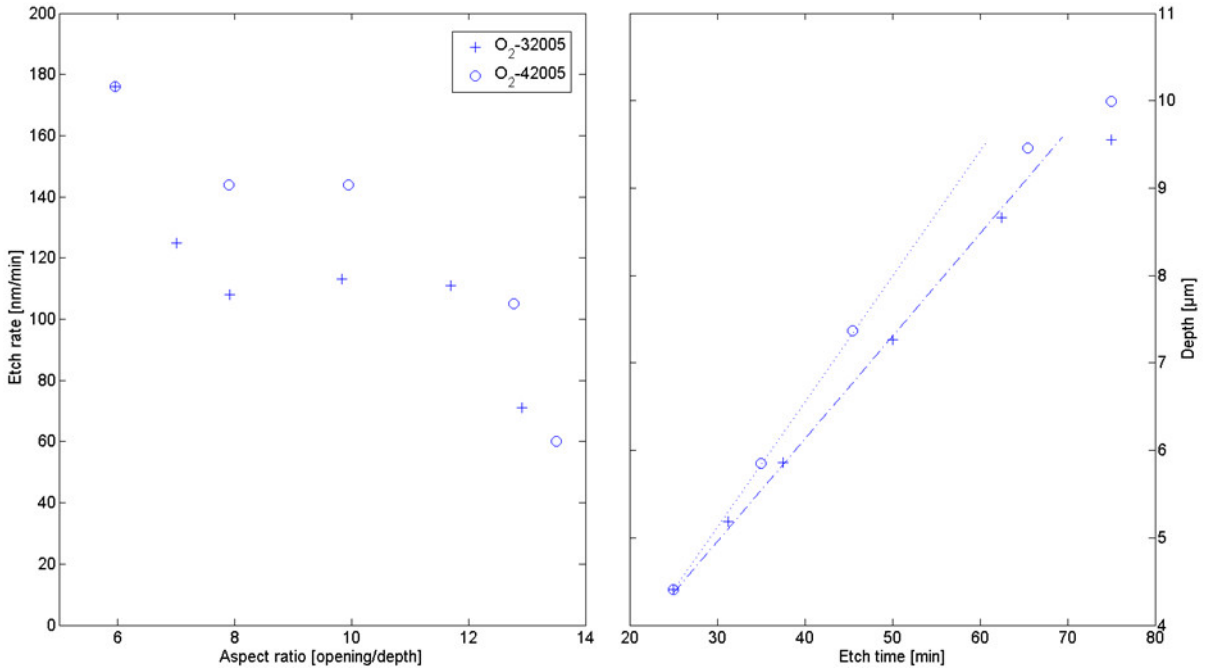

Figure 10: Plot of the aspect ratio versus the etch rate and etch depth versus the etch time using O_2-32005 and O_2-42005.

Table 4: Etch results for the iterative etching tests

Etch parameters	Top [nm]	Bottom [nm]	Depth [nm]	Angle [degrees]	Etch time [min]	Etch rate [nm/min]	Aspect ratio
O2-32005	681±11	1035±19	4409±45	2.30±0.18	25	176	5.56
O2-32005	677±13	1207±21	5190±97	2.92±0.17	31.25	125	7.01
O2-32005	657±7	1259±32	5864±53	2.94±0.16	37.5	108	5.86
O2-32005	680±16	1275±21	7272±25	2.34±0.09	50	113	9.83
O2-32005	687±11	1300±16	8658±34	2.03±0.05	62.5	111	11.70
O2-32005	686±8	1269±37	9550±95	1.75±0.11	75	71	12.91
O2-42005	687±11	1205±16	5849±84	2.54±0.11	35	144	7.90
O2-42005	684±9	1288±17	7365±58	2.11±0.10	45.5	144	9.95
O2-42005	680±13	1214±63	9458±81	1.62±0.13	65.5	105	12.78
O2-42005	684±10	1225±27	9993±61	1.55±0.08	75	60	13.50

4. Conclusion

We introduce the use of SAMIM for precise replications of short period resist gratings on top of small diamond substrates.

By changing the substrate bias power and the process pressure, and by using either pure O_2 or a mixture of Ar/O_2 plasma chemistries, it was possible to control the angle of the sidewalls between 2.1° to 4.2° in our etched diamond gratings.

We also demonstrate a new technique to reach even greater etch depth for a diamond optical grating by sputtering a fresh Al mask onto the already etched diamond grating and proceeding with a short Al etch step followed by diamond plasma etching. An aspect ratio of 13.5 was demonstrated for a grating with a period of 1.42 μm. Moreover, a sidewall angle as low as 1.55° was reached using this technique.

Finally, these findings will aid the fabrication of gratings, such as half wave plates based on subwavelength gratings, for which a good control of the grating parameters becomes extremely important to provide good optical performance.

Prime novelty statement

Lowest reported angle in high aspect diamond etching – 2.1° and leading aspect ratio of 1:8.

Lowest reported angle in high aspect diamond etching using re-sputtering – 1.55° with an aspect ratio of 1:13.5.

Acknowledgments

The authors gratefully acknowledge funding from the European Research Council under the European Union's Seventh Framework Programme (ERC Grant Agreement no. 337569).

References

[1] R. S. Balmer, J. R. Brandon, S. L. Clewes, H. K. Dhillon, J. M. Dodson, I. Friel, P. N. Inglis, T. D. Madgwick, M. L. Markham, T. P. Mollart, N. Perkins, G. a Scarsbrook, D. J. Twitchen, a J. Whitehead, J. J. Wilman, and S. M. Woollard, "Chemical vapour deposition synthetic diamond: materials, technology and applications.," *J. Phys. Condens. Matter*, vol. 21, no. 36, p. 364221, Sep. 2009.

[2] P. Forsberg and M. Karlsson, "High aspect ratio optical gratings in diamond," *Diam. Relat. Mater.*, vol. 34, pp. 19–24, Apr. 2013.

[3] C. Ribbing, P. Rangsten, and K. Hjort, "Diamond membrane based structures for miniature X-ray sources," *Diam. Relat. Mater.*, vol. 11, no. 1, pp. 1–7, Jan. 2002.

[4] M. Karlsson and F. Nikolajeff, "Diamond micro-optics: microlenses and antireflection structured surfaces for the infrared spectral region," *Opt. Express*, vol. 11, no. 5, p. 502, Mar. 2003.

[5] H. Uetsuka, T. Yamada, and S. Shikata, "ICP etching of polycrystalline diamonds: Fabrication of diamond nano-tips for AFM cantilevers," *Diam. Relat. Mater.*, vol. 17, no. 4–5, pp. 728–731, Apr. 2008.

[6] C. L. Lee, E. Gu, M. D. Dawson, I. Friel, and G. a. Scarsbrook, "Etching and micro-optics fabrication in diamond using chlorine-based inductively-coupled plasma," *Diam. Relat. Mater.*, vol. 17, no. 7–10, pp. 1292–1296, Jul. 2008.

[7] T. Yamada, H. Yoshikawa, H. Uetsuka, S. Kumaragurubaran, N. Tokuda, and S. Shikata, "Cycle of two-step etching process using ICP for diamond MEMS applications," *Diam. Relat. Mater.*, vol. 16, no. 4–7, pp. 996–999, Apr. 2007.

[8] D. T. Tran, T. A. Grotjohn, D. K. Reinhard, and J. Asmussen, "Microwave plasma-assisted etching of diamond," *Diam. Relat. Mater.*, vol. 17, no. 4–5, pp. 717–721, Apr. 2008.

[9] F. Silva, R. S. Sussmann, F. Bénédic, and A. Gicquel, "Reactive ion etching of diamond using microwave assisted plasmas," *Diam. Relat. Mater.*, vol. 12, no. 3–7, pp. 369–373, Mar. 2003.

[10] J. Evtimova, W. Kulisch, C. Petkov, E. Petkov, F. Schnabel, J. P. Reithmaier, and C. Popov, “Reactive ion etching of nanocrystalline diamond for the fabrication of one-dimensional nanopillars,” *Diam. Relat. Mater.*, vol. 36, pp. 58–63, Jun. 2013.

[11] D. S. Hwang, T. Saito, and N. Fujimori, “New etching process for device fabrication using diamond,” *Diam. Relat. Mater.*, vol. 13, no. 11–12, pp. 2207–2210, Nov. 2004.

[12] J. S. Hodges, L. Li, M. Lu, E. H. Chen, M. E. Trusheim, S. Allegri, X. Yao, O. Gaathon, H. Bakhru, and D. Englund, “Long-lived NV - spin coherence in high-purity diamond membranes,” *New J. Phys.*, vol. 14, 2012.

[13] C. Delacroix, P. Forsberg, M. Karlsson, D. Mawet, O. Absil, C. Hanot, J. Surdej, and S. Habraken, “Design, manufacturing, and performance analysis of mid-infrared achromatic half-wave plates with diamond subwavelength gratings,” *Appl. Opt.*, vol. 51, no. 24, p. 5897, 2012.

[14] E. Kim, Y. Xia, X. M. Zhao, and G. M. Whitesides, “Solvent-Assited Microcontact Molding: A Convenient Method for Fabricating Three-Dimensional Structures on Surfaces of Polymers,” *Adv. Mater.*, vol. 9, no. 8, pp. 651–654, 1997.

[15] M. Karlsson, K. Hjort, and F. Nikolajeff, “Transfer of continuous-relief diffractive structures into diamond by use of inductively coupled plasma dry etching.,” *Opt. Lett.*, vol. 26, no. 22, pp. 1752–1754, 2001.

[16] F. Nikolajeff and M. Karlsson, “Refractive and Diffractive Diamond Optics,” in *Optical Engineering of Diamond*, R. P. Mildren and J. R. Rabeau, Eds. Wiley-VCH, 2013, pp. 109–142.

[17] W. Eckstein, “Sputtering yields,” *Vacuum*, vol. 82, no. 9, pp. 930–934, 2008.

[18] Z. L. Zhang and L. Zhang, “Anisotropic angular distribution of sputtered atoms,” *Radiat. Eff. Defects Solids*, vol. 159, no. 5, pp. 301–307, 2004.